

Attempts to Produce Element 110 in Fusion Reactions of ^{40}Ar with $^{233,235,238}\text{U}$ ^B

K. Sümmerer, W. Bröchle, E. Jäger, K. J. Moody*, M. Schädel, G. Wirth,
(GSI Darmstadt)

U.W. Scherer, C. Frink, G. Herrmann, J.V. Kratz, N. Trautmann (Univ. Mainz)
H. Gäggeler (EIR Wuerenlingen)

The surprising stability against spontaneous fission that allowed the observation of α -decay for $^{265}_{108}$ and $^{260,261}_{106}$ in cold fusion reactions at SHIP^{1,2} has stimulated the idea that α -decay may also prevail for element 110. Even though the first attempt to fuse ^{64}Ni with ^{208}Pb was not successful³, there is hope that in the reaction of Ar + U one could benefit from a reduced hindrance for fusion as compared to the Ni + Pb case. On the other hand, the less favourable Q-values lead to higher excitation energies (of the order of 40 MeV) in the Ar + U reaction. We have therefore performed radiochemical searches for descendants of the 3n- and 4n- evaporation residues from bombardments of $^{233,235,238}\text{U}$ with ^{40}Ar at energies close to the Coulomb barrier. The predicted α -decay chains are compiled in the Table. To search for short-lived members of these chains, we have used thin targets of ^{233}U or ^{235}U in connection with a He-KCl-jet and the rotating catcher wheel ROMA⁴. Long-lived decay products were searched for in an off-line chemistry experiment where targets of ^{233}U , ^{235}U and ^{238}U on thick Be-backings were irradiated for 20 hours, typically. After that, the recoil catchers were chemically separated into various actinide fractions and assayed for α - and sf-decay.

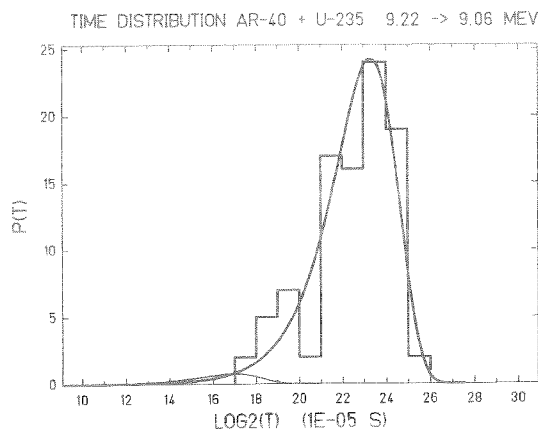
In the ROMA experiment the α -spectra up to 9 MeV showed large activities of known short-lived transfer-products and/or their daughter products obscuring Table:

Tentative decay chains of Ar(U,3n) and Ar(U,4n) channels. Nuclei in boxes were searched for in this experiment.

ER product	decay products			
$^{233}\text{U}, 3n$	$^{270}_{110}$ 7.3 ms ^a 10.24 MeV ^b	$^{266}_{108}$ 130 ms ^a 9.56 MeV ^b	$^{262}_{106}$ 97 ms ^a 9.38 MeV ^b	$^{258}_{104}$ 13 ms sf
$^{233}\text{U}, 4n$	$^{269}_{110}$ 5.2 ms ^a 10.44 MeV ^b	$^{265}_{108}$ 1.8 ms ^a 10.36 MeV ^b	$^{261}_{106}$ 260 ms 9.56 MeV...	$^{257}_{104}$ 4.3 s 8.98 MeV... $^{255}_{103}$ 1.7 m 8.01 MeV $^{249}_{101}$ 2.6 m 7.53 MeV
$^{235}\text{U}, 3n$	$^{272}_{110}$ 220 ms ^a 9.70 MeV ^b	$^{268}_{108}$ 5.5 s ^a 9.01 MeV ^b	$^{264}_{106}$ 7.8 s ^a 8.76 MeV ^b	$^{260}_{104}$ 21 ms sf
$^{235}\text{U}, 4n$	$^{271}_{110}$ 200 ms ^a 9.92 MeV ^b	$^{267}_{108}$ 4.7 s ^a 9.22 MeV ^b	$^{263}_{106}$ 0.9 s 9.06 MeV 9.23 MeV	$^{259}_{104}$ 3 s 8.77 MeV 8.86 MeV $^{255}_{103}$ 3.1 m 8.12 MeV 7.33 MeV $^{255}_{102}$ 27 m 7.02 MeV
$^{238}\text{U}, 3n$	$^{275}_{110}$ 1.3 ms ^a 10.9 MeV ^b	$^{271}_{108}$ 38 ns ^a 8.54 MeV ^b	$^{267}_{106}$ 2.2 d ^a 7.81 MeV ^b	$^{263}_{104}$ 32.5 h ^a 7.64 MeV ^b $^{259}_{103}$ 58 m 7.50 MeV $^{255}_{101}$ 20.1 h 7.02 MeV
$^{238}\text{U}, 4n$	$^{274}_{110}$ 5 ms ^a 10.3 MeV ^b	$^{270}_{108}$ 4.2 h ^a 8.51 MeV ^b	$^{266}_{106}$ 12.6 d ^a 8.18 MeV ^b	$^{262}_{104}$ 47 ms sf

^aPoenaru & Ivascu, Ref.5

^bLeander et al., Ref.6



many of the predicted α -lines. Sensitive indicators for Ar + U-evaporation residues according to the predictions are the sf-decay of $^{260}_{104}$ (from $(^{235}\text{U},3n)$) or time-correlated α -events of $^{267}_{108}$ - $^{263}_{106}$ (from $(^{235}\text{U},4n)$). We have observed no fissions with ^{235}U and one sf-event with the ^{233}U target, which corresponds to a cross section limit of 0.9 nb. With the ^{235}U target, we have obtained the time distribution of 9.2 - 9.06 MeV α - α -correlations shown in the Figure. All events can be interpreted as random. We deduce an upper limit of 0.8 nb for the $(^{235}\text{U},4n)$ -channel from these results.

For the chemical search for long lived descendants of element 110 isotopes it was necessary to show that these nuclides are not formed in transfer reactions. We found that the cross sections for transuranium isotopes decrease very steeply beyond Cf such that only upper limits for the cross sections of Es, Fm and Md isotopes could be determined. Among these is also the descendant of the $(^{235}\text{U},4n)$ and the $(^{238}\text{U},3n)$ channel, ^{255}Fm . Due to EC branchings, ^{255}Fm is formed with probabilities of 32.5% and 78%, respectively. From the non-observation of this isotope we deduce upper limits of 1.2 nb for the $(^{235}\text{U},4n)$ reaction and 3.9 nb for the $(^{238}\text{U},3n)$ reaction.

References:

1. G. Münzenberg et al., Z. Phys. A317 (1984) 235
2. F. P. Heßberger et al., Z. Phys. A322 (1985) 227
3. G. Münzenberg et al., contribution to this Report
4. K. Sümmerer et al., Proc. XII Int. Winter Meeting on Nucl. Phys., Bormio, Italy (1984)
5. D. N. Poenaru et al., J. Physique 44 (1983) 791
6. G. A. Leander et al., Proc. AMCO-7 (1984) 466

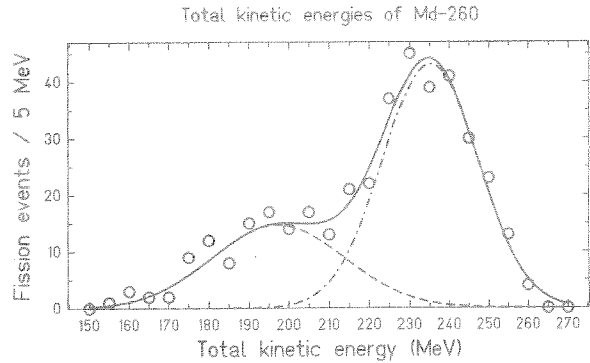
* Present address: L-232, Lawrence Livermore Nat. Lab., Livermore, USA

Bimodal Symmetric Fission Observed in the Heaviest Elements

E. K. Hulet, J. F. Wild, R. J. Dougan, R. W. Lougheed, J. H. Landrum,
 A. D. Dougan, P. A. Baisden, C. M. Henderson, R. J. Dupzyk
 (LLNL Livermore)
 M. Schädel, K. Sümmerer (GSI Darmstadt)
 R. L. Hahn (ORNL Oak Ridge), G. Bethune (Daytona Beach)

The availability of ^{254}Es -targets and the high production rates of n-rich isotopes of the heaviest elements in light-ion induced transfer reactions¹ have made feasible searches for new and more detailed studies of known sf-emitters like ^{258}Fm or ^{259}Md . For these isotopes a transition to symmetric mass division has been observed previously^{2,3}. To circumvent the interference of ^{256}Fm which is abundantly produced in these reactions, an experiment was performed which utilized off-line mass separation as the key technique^{4,5}. A ^{254}Es target of 1.1×10^{17} atoms/cm² was bombarded with beams of 105 MeV ^{18}O or 126 MeV ^{22}Ne from the 88" cyclotron at the LBL. Recoil products were trapped in 3.6 mg/cm² Ta foils which were flown by helicopter to the LLNL for mass separation. Measurement of α - and sf-decay of the mass separated samples started typically one hour after the end of bombardment. Consequently, we were able to detect the sf-activities from the EC decay of 60-min ^{258}Md into ^{258}Fm and from 95 min ^{259}Md . In addition, a hitherto unknown sf-emitter was found in the A=260 fraction with the remarkably long half-life of 32 days which was formed with a cross section of 0.3 μb in both reactions. Extrapolating the cross sections from earlier experiments¹ to A=260 and taking into account the long half-life we could assign this activity to ^{260}Md .

An interesting aspect of this new sf-emitter is the TKE-distribution shown in the Figure. As with $^{258,259}\text{Fm}$, a high-TKE component is visible which corresponds to an extremely narrow symmetric mass distribution. A hitherto unobserved feature is the clear indication of a second also symmetric low-TKE component



corresponding to broad wings in the mass distribution. The most probable TKE of this second component (195 MeV) is compatible with the empirical systematics of Viola et al.⁶. Unexpectedly, the feature of "bimodal symmetric fission" in the same nucleus seems to be present also in the TKE-distributions of other heavy nuclei⁵ where insufficient statistics had prevented such an observation up to now.

Table 1 lists the sf-properties of ^{258}Fm and $^{259,260}\text{Md}$ from our experiments together with those for ^{258}No and $^{260}\text{104}$ from earlier studies with the SWAMI system^{7,8}. All mass-distributions are symmetric except for, possibly, the low-TKE component of ^{259}Md where the present level of statistics indicates an asymmetric mass-distribution.

At present only a qualitative interpretation of our results is at hand. Whereas the low-TKE component confirms the trend observed for lighter nuclei⁶ and may be termed "liquid-drop like fission", the high-TKE component appears to be governed by shell-effects in the nascent fragments^{2,9}. The detailed interplay between the two fission modes and the preference of symmetric or asymmetric mass splits, respectively, has not yet been explored theoretically, however.

Table 1: Proposed decomposition of the TKE-spectra of sf-emitters with $Z \geq 100$ into two components

sf-emitter	low TKE			High TKE		
	<TKE> (MeV)	FWHM ^C (%)	%	<TKE> (MeV)	FWHM (%)	%
^{258}Fm	205	45	44%	232	26	56%
^{259}Md	201	45	85%	235	19	15%
^{260}Md	195	45	35%	234	32	65%
$^{258}\text{No}^a$	203	45	91%	235	18	9%
$^{260}\text{104}^b$	197	45	100%	-	-	-

^aRef.7 ^bRef.8 ^cfixed to value for $^{260}\text{104}$

References:

1. M. Schädel et al., GSI-Preprint 85-30 (1985), submitted to Phys. Rev. C.
2. D.C. Hoffmann et al., Phys. Rev. C21 (1980) 972
3. J.F. Wild et al., Phys. Rev. C26 (1982) 1531
4. R. W. Lougheed, Proc. of the Actinides 85-Conference, Aix en Provence, 1985.
5. E. K. Hulet et al., preprint UCRL-93218, 1985, submitted to Phys. Rev. Lett.
6. V.E. Viola, Nucl. Data 1 (1966) 391
7. J. F. Wild et al., LLNL Nucl. Chem. Div. Ann. Rep. FY-84, UCAR-10062-84/1, 6-23 (1984)
8. E. K. Hulet et al., LLNL Nucl. Chem. Div. Ann. Rep. FY-82, UCAR-10062-82/1, 98 (1982)
9. U. Mosel, H.W. Schmitt, Phys. Rev. C4 (1971) 2185

Identification of the New Nuclides ^{243}Np and ^{244}Np G

H. Tetzlaff, G. Herrmann*, N. Kaffrell, J.V. Kratz, J. Rogowski, N. Trautmann
Institut für Kernchemie, Universität Mainz

K.J. Moody, W. Brüchle, M. Brügger, H. Gäggeler[†], M. Schädel, K. Sümmerner
GSI Darmstadt

M. Skalberg, G. Skarnemark
Chalmers University of Technology, Göteborg

M.M. Fowler
Los Alamos National Laboratory

J. Alstad
Department of Chemistry, University Oslo

In the collision between ^{136}Xe and ^{244}Pu neutron-rich actinide isotopes are formed by few nucleon transfer. A target of $770 \mu\text{g}/\text{cm}^2$ ^{244}Pu was irradiated with ^{136}Xe ions of 6.15 MeV/u energy. For the chemical isolation of neptunium from the reaction products two different automated procedures in combination with a gas-jet transport system were used. The reaction products recoiling out of the target were thermalized in argon gas loaded with KCl-clusters and transported through a capillary to either the SISAK¹ or the ARCA² chemistry systems.

With the centrifuge-system SISAK II the neptunium fraction was separated on-line by multistage liquid-liquid extraction as described earlier³. In the last step neptunium was back-extracted from the organic phase with hot phosphoric acid. The whole procedure takes about 10 s. Two methods were used for the half-life determination: In the first, the four-detector delay method, the activity in the phosphoric acid was pumped on-line through a long teflon tube and measured with four Ge-detectors connected in series. The flow-rate of the phosphoric acid was kept constant. Two runs with different delay tubes between the detectors were performed. The half-lives of the neptunium isotopes were determined from the decrease of the count-rate of the corresponding γ -lines in the four detectors as a function of the delay time. In the second method the phosphoric acid was pumped through a 1.8 ml column filled with hydrated antimony pentoxide. Neptunium is absorbed on the column and the decay of the neutron-rich isotopes was measured off-line.

In the ARCA experiments the separation of neptunium was accomplished batchwise. The reaction products attached to the clusters were collected for 15 min on a glass frit, dissolved in concentrated nitric acid and absorbed on an anion exchange column. After elution neptunium was purified by an extraction step with tri-n-octylamine (TOA). The procedure was performed within 2.5 min.

As a result from the experiments a γ -line at 287 keV

could be assigned to the ^{243}Np -decay and γ -lines at 163, 217, and 681 keV to the decay of ^{244}Np . The assignments are based on known excited states in the plutonium daughter nuclei. From the decay of the γ -lines half-lives of 1.8 ± 0.3 min and 2.5 ± 0.3 min were determined for ^{243}Np and ^{244}Np , respectively, as shown in Figs. 1 and 2.

* also at GSI Darmstadt

† presently at EIR Würenlingen

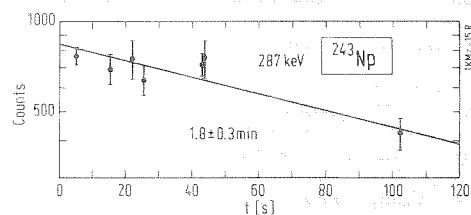


Fig. 1: Decay of the 287 keV γ -line of ^{243}Np (SISAK data)

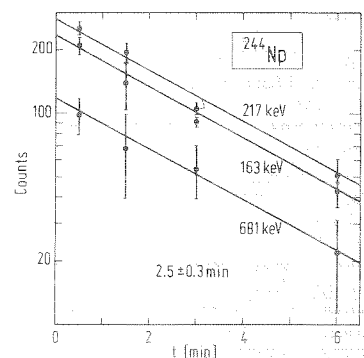


Fig. 2: Decay of the γ -lines at 163, 217, and 681 keV of ^{244}Np (ARCA data).

References

- 1 G. Skarnemark et al., Nucl. Instr. Meth. 171, 323 (1981)
- 2 W. Brüchle et al., GSI Scientific Report 1983, GSI 84-1, p. 247 (1984)
- 3 H. Tetzlaff et al., GSI Scientific Report 1984, GSI 85-1, p. 273 (1985)

Excitation functions for the production of below-target nuclides
in transfer reactions of ^{136}Xe with ^{238}U , $^{239,244}\text{Pu}$ and ^{186}W

R. Schmoll, J.V. Kratz, H. Keller, S. Zauner
Institut für Kernchemie, Universität Mainz

A. Türler*, H. Gäggeler*, H.R. von Gunten*, F. Wegmüller*
*Universität Bern, *E.I.R. Würenlingen

K.J. Moody, W. Brüche, M. Brügger, M. Schädel, K. Sümmerer, G. Wirth
GSI Darmstadt

The use of transfer reactions between complex nuclei for the production and study of new, neutron-rich isotopes is now well established ¹⁻⁵. To characterize the relevant reaction channels we have studied cross section systematics ⁶ and excitation functions for ^{136}Xe -induced reactions with ^{238}U , $^{239,244}\text{Pu}$ and with ^{186}W . Target-like recoils were collected with Cu-catcher foils, chemically separated ⁶, and counted for γ -ray activities.

For $^{136}\text{Xe} + ^{186}\text{W}$ the isotopic distributions of the elements tantalum, hafnium, and lutetium exhibit a very broad dispersion extending to very neutron-deficient nuclei due to deep-inelastic reactions followed by neutron evaporation, which merges, on the neutron-rich side, into a narrow distribution of quasielastic transfer products with mass numbers close to that of the target. For $^{136}\text{Xe} + \text{U, Pu}$ the broad deep-inelastic products distribution is less pronounced, or missing, which is probably caused by sequential fission. On the other hand, for products with mass numbers close to the target we observe essentially the same cross sections as in the $^{136}\text{Xe} + ^{186}\text{W}$ reaction. These are of the order of 100 mb for 1n-stripping and 1n-pick-up, about 10-15 mb for 1p-stripping from the target, and 2-10 mb for 2p-stripping from the target. The cross sections for the 2p-stripping channel decrease regularly with increasing neutron excess of the target (^{239}Pu , ^{238}U , ^{244}Pu) in qualitative agreement with potential energy considerations.

Consistent with the association of narrow product distributions with mass numbers close to the target mass number to quasi-elastic transfer, we observe for these products excitation functions that are essentially flat above the barrier ⁷, see Fig.1. For increasing mass loss ΔA of the target-like product (increasing nucleon exchange, energy dissipation and particle evaporation) there is a regularly increasing tendency of the excitation functions to rise. This is the expected feature for deep-inelastic collisions. For reactions with the actinide targets examples for the energy dependence of the cross sections are shown in Fig.2. The slight decrease of the cross sections (which has previously been seen in similar reactions with ^{238}U and ^{248}Cm targets) is most likely due to increasing energy dissipation and associated losses of yield due to sequential fission as the available energy above the barrier increases.

These results establish the following optimum conditions for the production and study of new neutron-rich products from transfer reactions with ^{136}Xe : For the ^{186}W target incident energies well above the barrier (10 MeV/u) and thick ($\leq 20 \text{ mg/cm}^2$) targets should be used. The optimum bombarding energies for actinide targets are about 10% above the barrier.

References:

- ¹ R. Kirchner et al., Nucl. Phys. **A378**, 549(1982)
- ² K. Rykaczewski et al., Z. Phys. **A309**, 273(1983)
- ³ E. Runte et al., Nucl. Phys. **A399**, 163(1983)
- ⁴ K.-L. Gippert et al., GSI Scientific Report 1984, p.96
- ⁵ K.J. Moody et al., GSI Scientific Report 1984, p.93
- ⁶ A. Türler et al., GSI Scientific Report 1984, p.95
- ⁷ D. Gardes et al., Phys. Rev. **C18**, 1298(1978)

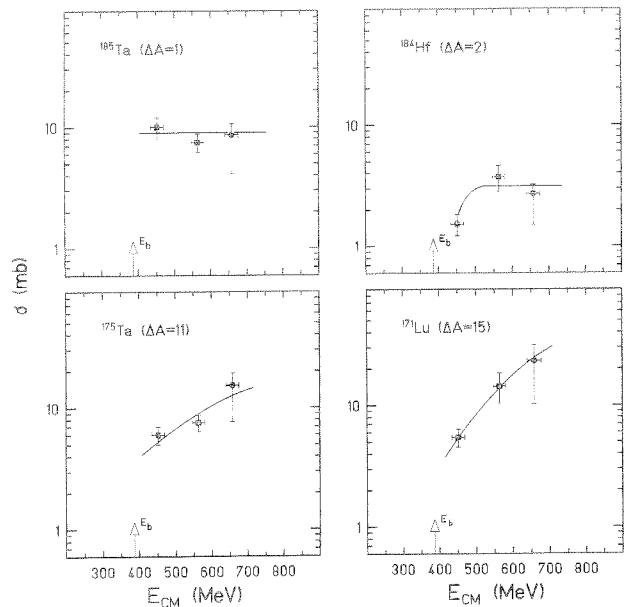


Fig.1: Energy dependence of the cross section for formation of selected below-target products in the $^{136}\text{Xe} + ^{186}\text{W}$ reaction. The curves are drawn to guide the eye.

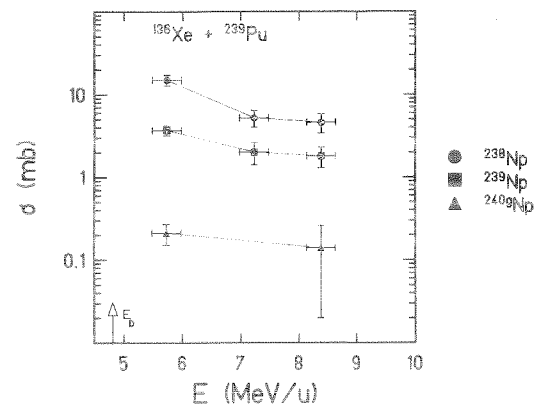


Fig.2: Same as Fig.1 for the $^{136}\text{Xe} + ^{239}\text{Pu}$ reaction.

²⁰³B
Search for the decay of ²⁰³Au

W. Brüche (GSI Darmstadt), R. Bellwied (Inst. f. Kernchemie, Uni Mainz)

²⁰³Au is the only nucleus in the direct vicinity of stable nuclei where one does not know any decay properties. The chart of nuclides shows only an empty blue field. There exist only three publications dealing with this subject, with questionable results¹⁻³. After irradiation of Hg with fast neutrons Butement¹ assigned a 55s activity to ²⁰³Au, but neither ²⁰²Au ($T_{1/2}=28s$), nor ²⁰⁴Au ($T_{1/2}=40s$), which are produced as main activities, were found. Bunus² used the same reaction and found a line at 0.69MeV (NaJ- detector) which he assigned to ²⁰³Au. This line seems now clearly to stem from the decay of ²⁰⁴Au (691.7keV + 723.0keV). Naim³ found γ -lines (618 \pm 1keV, $T_{1/2}=3h$; 300keV, $T_{1/2}=7h$) which have a striking similarity to the well known γ -lines of ¹¹²Ag and ¹¹³Ag. This can easily be explained by contaminations of their targets with Cd.

We used the Mainz Cockcroft- Walton Accelerator to search for ²⁰³Au by the reaction ²⁰⁴Hg(n,d)²⁰³Au. Because we used targets of natural mercury nitrate, other short lived gold isotopes are produced by (n,p)-reactions. To avoid interference from Hg- and Pt-isotopes we carried out a chemical separation based on the extraction of Au in Tributylphosphate (TBP). After 2 min irradiation with 4.5×10^{10} 14MeV neutrons / (cm²s) the target samples were transported to the laboratory by a fast pneumatic system. The capsules were opened and the powdered Hg(NO₃)₂ was dissolved in hot HCl. Now the solution was succed through a column of TBP absorbed on Voltalef®. After washing with 3n HCl the TBP could be ejected into a thin polystyrene box and assayed for γ - and X-ray singles and coincidences. Two spectra are shown in Figs.1+2. Time from end of irradiation to start of measurement was 30s, the contaminations from the main reaction product ^{199m}Hg are less than 10⁻⁴. Except for one γ -line at 26.3keV ($T_{1/2}$ 2min) all observed lines could be assigned to the decay of known nuclides. Two other new lines at 196keV and 388keV fit to the decay of ²⁰²Au. Below 375keV until now no one had observed γ -lines of ^{202,204}Au, because the huge activities of Hg without chemical separation obscured all other reaction products^{4,5}.

There are three possibilities why we could not detect ²⁰³Au:

a) The cross section for the (n,d)-reaction is too small. This is unlikely; we even saw ^{195m}Au which is produced from ¹⁹⁶Hg with 0.15% natural abundance, compared to 6.8% of ²⁰⁴Hg.

b) There is only ground- state to ground- state β^- -decay. To check this we made 10 milking experiments and separated 4 fractions of Hg grown from Au with a delay of 20s between each milking. No ²⁰³Hg could be detected after 2 weeks of measuring in shielded detectors.

c) The half-live is below 10s. This is the most probable reason. Possibly the 4s activity observed by Ward⁶ is ²⁰³Au. To check this an on- line chemistry experiment with a centrifuge system would be advisable.

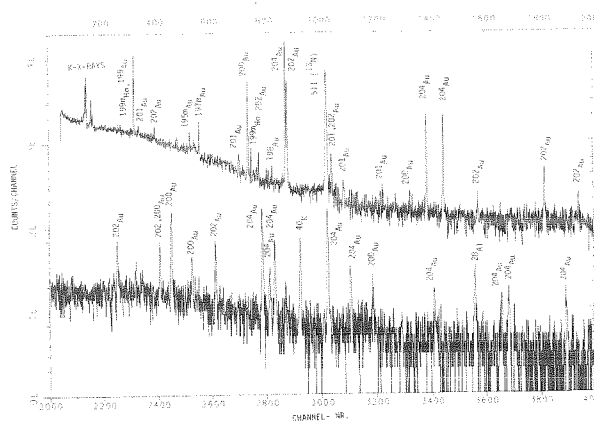


Fig.1 γ -spectrum of a Au fraction after irradiation of nat.Hg with 14MeV neutrons. (The upper part of the spectrum was multiplied by 5).

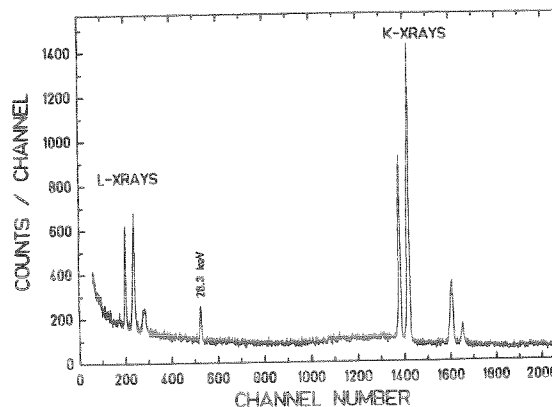


Fig.2 X-Ray-spectrum of a Au fraction after irradiation of nat.Hg with 14MeV neutrons.

References:

1. F.D.S. Butement, R. Shillito, Proc.Phys.Soc. **65A** (1952), 945
2. F.T. Bunus, Radioch. Acta **18** (1972), 192
3. M.A.Naim, A.Szalay, Radiochem. Radioanal. Lett. **37** (1979), 45
4. A. Pakkanen et.al., Nucl. Phys. **A184** (1972), 157
5. D.A. Craig, H.W. Taylor, J. Phys. **G 10** (1984), 1133
6. T.E. Ward et.al., Phys. Rev. **164** (1967), 1545

Sub-Coulomb Transfer in Heavy-Ion Collisions ^B

G. Wirth, W. Brüche, K. Sümmerer
 GSI Darmstadt
 F. Funke, J.V. Kratz, M. Lerch, N. Trautmann
 Institut für Kernchemie, Universität Mainz

Angular distributions of the quasi-elastic 1n-transfer product ^{239}U had previously been measured in the reaction $^{238}\text{U} + ^{238}\text{U}$ at energies below the Coulomb barrier from 90° to 45° in the laboratory system ¹. The transfer probabilities for the more central collisions showed deviations from a semiclassical description. We could not exclude that the observed deviations originate from angular straggling in the target of the projectile-like transfer products, which have very low laboratory velocities in this symmetric reaction. Therefore we measured in addition the transfer product ^{239}U in the angular range $\theta_{\text{Lab}} = 45^\circ - 5^\circ$ with better angular resolution compared to the earlier experiments at backward angles. Although there is a small experimental problem for the most central collisions the angular distributions are in general symmetric around $\theta_{\text{CM}} = 90^\circ$ as expected from trivial kinematics. A summary of the data is given in ref. [2]. For the peripheral collisions the transfer probabilities behave as expected from a semiclassical approach, whereas significantly lower transfer probabilities are observed for the more central collisions. The difference between the integrated experimental angular distribution and the theory amounts roughly to 70% of the measured cross sections at the lower beam energies and is 36 mb compared to the measured integral cross section of 48 mb at 5.65 MeV/u.

In order to check whether the transfer cross section is reduced by sequential fission after transfer we measured the excitation function of the fission component (fig.1). The integral fission cross section for the reaction $^{238}\text{U} + ^{238}\text{U}$ at $E_{\text{lab}} = 5.65$ MeV/u is about 25 mb and can be assigned completely to Coulomb fission calculated to be 23 mb ³. Therefore the fission component cannot accommodate 36 mb from transfer fission.

The general shape of the observed transfer angular distributions is similar to the prediction of a schematic model ⁴ including long contact times associated with a potential pocket at energies below the barrier. However this similarity is not a proof for the existence of such a pocket as long as simpler explanations have not been ruled out. Coulomb excitation is a strong process in $^{238}\text{U} + ^{238}\text{U}$ collisions. A dependence of the transfer probability on the rotational state populated in the collision has not been taken into account yet. To provide further insight similar experiments with other deformed and spherical heavy nuclei are necessary.

Along that line we have investigated the symmetric reaction $^{197}\text{Au} + ^{197}\text{Au}$ involving nearly spherical heavy ions. The angular distributions were measured for the 1n-transfer products $^{198g,m}\text{Au}$, $^{196g,m2}\text{Au}$ and for the 2n-transfer product ^{199}Au at beam energies of 5.06 ($0.88 \times B$) and 5.35 ($0.93 \times B$) MeV/u (fig.2). Data analysis is still in progress but it seems that the transfer probabilities are compatible with the semiclassical expectation at all angles and do not show deviations for the more central collisions as observed in $^{238}\text{U} + ^{238}\text{U}$.

Products from many-nucleon transfer are found in the reaction $^{238}\text{U} + ^{238}\text{U}$ at 5.85 MeV/u ($0.96 \times B$) with small cross sections ¹. A rough angular distribution was measured for ^{227}Th (2p9n-transfer). Although the shape of the angular distribution is steeper compared to that of the 1n-transfer product ^{239}U the ^{227}Th was measurable at $\theta_{\text{Lab}} \approx 45^\circ$ with a differential cross section of about $0.2 \mu\text{b/sr}$.

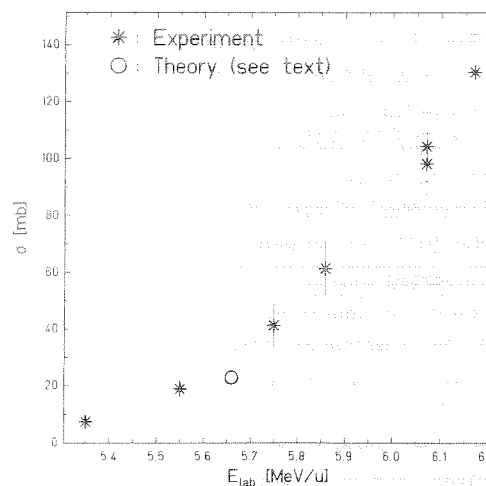


Fig.1
 Excitation function of fission in the reaction $^{238}\text{U} + ^{238}\text{U}$. The crosses are the experimental data points, the circle is the calculated value for Coulomb fission.

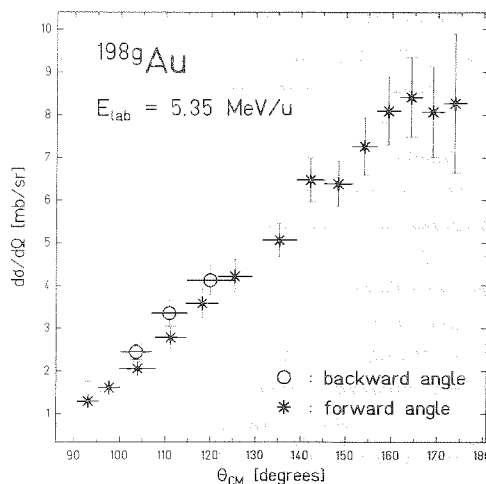


Fig.2
 Angular distribution of ^{198g}Au in the reaction $^{197}\text{Au} + ^{197}\text{Au}$ at 5.35 MeV/u. The data are not yet corrected for contributions of target-like and beam-like ^{198g}Au , respectively. The horizontal bars indicate the experimental angular resolution.

References

1. G. Wirth et al., GSI 85-1, 29 (1985)
2. G. Wirth et al., GSI 85-64 (1985)
3. V.E. Oberacker, W. Pinkston and H. Kruse, Reports on Progress in Physics 48 (1985) 327
4. D.P. Russell, W.T. Pinkston and V.E. Oberacker, Phys.Lett. 158B (1985) 201

Binary reactions near the Coulomb barrier in systems with
dynamically hindered fusion

B

1.2.1

R. Bellwied, H. Keller, J.V. Kratz, K. Lützenkirchen
Institut für Kernchemie der Universität Mainz
W. Brüchele, L. Dörr, K.J. Moody, W. Reisdorf, M. Schädel,
K. Sümmerer, G. Wirth
GSI Darmstadt

The extra-push concept of Swiatecki et al.^{1,2} and recent experimental evidence^{3,4,5} experimental evidence for the hindrance of fusion into a true compound nucleus inside the fission saddle point, and for the hindrance of capture, respectively, have suggested the following view⁶: For undercritical systems the total reaction cross section consists of just two components - quasi elastic scattering plus transfer, and complete fusion. Upon an increase of projectile and/or target charge compound nucleus formation is suppressed and the quasi-fission reaction makes its appearance. Only upon a further increase of the charges becomes the less restrictive capture phenomenon (quasi-fission) hindered too, and is partly replaced by deep-inelastic scattering.

Most experimental evidence for quasi-fission was gained in extremely heavy systems with marginal final state stability. The present work aims at checking the above view⁶ also for lighter and nearly symmetric target-projectile combinations for which more stable compound nuclei exist. Mass and charge distributions were measured radiochemically in the reactions $^{86}\text{Kr} + ^{76}\text{Ge}$ ($x_{\text{eff}}=0.60$), $^{86}\text{Kr} + ^{104}\text{Ru}$ ($x_{\text{eff}}=0.70$), and $^{86}\text{Kr} + ^{130}\text{Te}$ ($x_{\text{eff}}=0.74$) at the barrier, thus testing the occurrence of the above mentioned, competing reaction channels in a system below, at, and slightly above the threshold ($x_{\text{thr}}=0.70$) for the hindrance of fusion. Evaluation of the $^{86}\text{Kr} + ^{104}\text{Ru}$ data is still in progress. For the other two systems, from the measured nuclide distributions⁶ we have constructed complete mass distributions which are shown in figs.1 and 2. The $^{86}\text{Kr} + ^{76}\text{Ge}$ reaction shows, besides fusion, only two sharply peaked distributions around target and projectile mass which are slightly skewed towards larger mass asymmetry. For $^{86}\text{Kr} + ^{130}\text{Te}$ these quasi-elastic peaks have nearly the same shape but are a factor of seven higher than in the lighter system. There are two more distinctly different features for $^{86}\text{Kr} + ^{130}\text{Te}$: i) the transfer peaks have tails on both sides, and ii) there is a relatively flat distribution filling the valley between the transfer peaks to the mb level. While i) might present some tentative evidence for deep-inelastic scattering, component ii) can be identified with quasi-fission. This is corroborated by the angular distributions. The total cross section that does not fit into the quasi elastic peaks is 30 mb. The contribution of true fusion-fission to the symmetric mass yield can be estimated on the basis of the results of Sahn et al.³ as 0.6 mb and is thus almost negligible.

For the cross section balance it was first of all interesting to discuss whether the factor of seven increase in the quasi-elastic transfer cross section indicated that the suppressed fusion cross section shows up in surface reactions. However, calculations of the 1n-transfer cross sections with the code PTOLEMY for $^{86}\text{Kr} + ^{76}\text{Ge}$, ^{130}Te reproduce this increase and its known continuation toward even heavier systems. Measurements⁹ with undercritical systems at higher incident energy also show this effect. It appears that the increasing surface confinement of the total reaction flux with increasing target/projectile mass or charge is a global phenomenon which does not show any particular structure at the threshold for the dynamical hindrance of fusion.

For the hypothetical case of unhindered fusion of $^{86}\text{Kr} + ^{130}\text{Te}$ we estimate a fusion cross section of roughly 30 mb. From the reappearance of this missing cross section in binary channels which span a range of 70 mass units we conclude that, even though fusion is suppressed, deep contact is being made. A differentiation of the massive transfer channels into quasi-fission and deep inelastic contributions is not possible on the basis of the present experimental data. Nevertheless, it is instructive to calculate the cross section for quasi-fission on the basis of the most recent extra-push parameterization by Töke et al.⁷ where $x_{\text{thr}}=0.70$ and the friction parameter \underline{a} resumes values of 7 or 10. This yields 15 mb or 25 mb for quasi-fission, respectively,

see fig.2. This would leave roughly 10 mb for deep inelastic scattering which is compatible with the cross section contained in the tails of the transfer peaks, see i) above.

¹ W.J. Swiatecki, Nucl. Phys. A376,471(1982)

² S. Bjørnholm et al., Nucl. Phys. A391,471(1982)

³ C. C. Sahn et al., Nucl. Phys. A441,316(1985)

⁴ R. Bock et al., Nucl. Phys. A388,334(1982)

⁵ B. B. Back, Phys. Rev. C31,2104(1985)

⁶ R. Bellwied et al., GSI Sci. Rep. 1984, p.35

⁷ J. Töke et al., Nucl. Phys. A440,327(1985)

⁸ K. E. Rehm et al., Phys. Rev. Lett. 51,1426(1983)

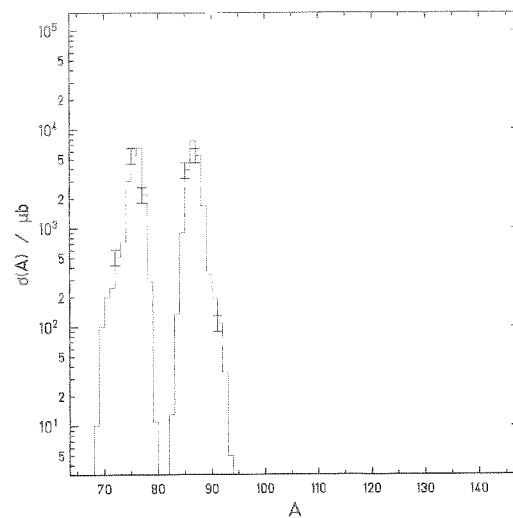


Fig.1; Mass distribution for the transfer reactions between $^{86}\text{Kr} + ^{76}\text{Ge}$ at 3.22 MeV/u in a histogram plot. Some representative error bars are shown.

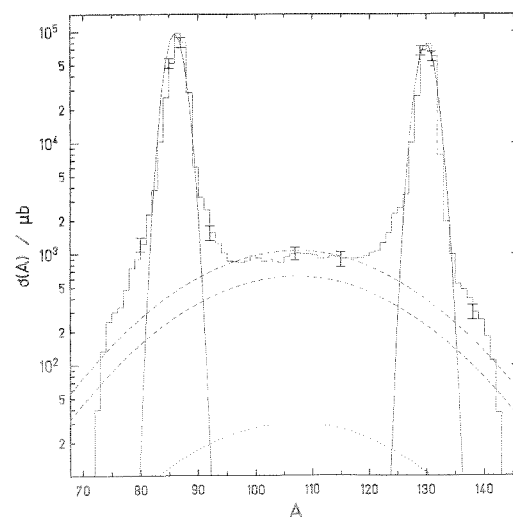


Fig.2: Mass distribution for binary reaction channels in the $^{86}\text{Kr} + ^{130}\text{Te}$ reaction at 3.96 MeV/u in a histogram plot. Typical error bars are shown. The quasi elastic peaks are overlaid by the shape of these peaks in the Kr + Ge-reaction (solid line). The dotted line is an estimate of the contribution of the compound nucleus fission to the symmetric mass yields based on the results of ref.3. The dashed lines represent estimates of the quasi-fission cross section with $x_{\text{thr}}=0.70$ and $a=7$ or $a=10$.

Angular Distributions in Quasi-Fission Reactions

K.Lützenkirchen* and J.V.Kratz, Institut für Kernchemie der Universität Mainz

G.Wirth, W.Brüchle, and K.Sümmerer, GSI Darmstadt

R.Lucas, J.Poitou, and C.Grégoire, DPHN-MF, CEN Saclay

Angular distributions of fission-like products in reactions of heavy projectiles ($Z_1=16-28$) with heavy target nuclei ($Z_2=79-92$) have recently been studied quite intensively /1,2,e.g./. In the region of heavy target-projectile combinations ($Z_1 \cdot Z_2 \geq 1600$) two competing processes can result in a complete relaxation of the relative kinetic energy and the mass asymmetry /3/: Fusion and compound-nucleus formation on the one hand, and quasi-fission on the other.

As reported previously /4/ skewed angular distributions $d^2\sigma/d\theta dZ$ (Fig.1) were measured in the reactions $^{50}\text{Ti} + ^{208}\text{Pb}$ at 5.0 and 5.5 MeV/u and $^{56}\text{Fe} + ^{208}\text{Pb}$ at 5.7, 6.1, 6.8, and 8.3 MeV/u. The skewness was interpreted as a clear signature of quasi-fission reactions which in turn proceed on a time scale comparable to the rotational period of the system.

The distributions can be described in the frame of a dynamical model /5,6/ (solid line in Fig.1), in which nucleon exchange is assumed to cause the excitation of a dinucleus' six intrinsic rotational modes. The tilting mode, a common rotation of the fissioning system around the dinuclear symmetry axis, is the only one which affects the angular distributions. In fact, its influence is manifest in the strongly decreasing cross section near 0° and 180° (Fig.1).

From the fits one obtains the variance of the tilting angular momenta for the forward (near 0°) and backward (near 180°) hemisphere, $K_0^2(\circ)$ and $K_0^2(\square)$, respectively /6/. In Fig.2 the square roots of these values are depicted as a function of fragment charge Z for $E/A=6.8$ MeV. In many cases, K_0 is smaller than the equilibrium value calculated in the frame of a scission-point model /6/ for two spheres in contact (solid line in Fig.2). Also, $K_0(\circ)$ and $K_0(\square)$, belonging to different reaction times, are usually quite different from each other. Both these findings indicate that the excitation of the tilting mode has not reached some kind of steady state related to an effective decision-point configuration.

In order to obtain a time scale for the excitation of K_0 , $d^2\sigma/d\theta dZ$ was unfolded into two gaussian distributions, one for the projectile, and one for the target contribution; the gaussians then depend on the rotation angle $\Delta\theta$ (Fig.3, for details see /6/). By minimization of χ^2 mean rotation angles were calculated for the projectile and the target contribution, $\langle\Delta\theta(Z)\rangle^p$ and $\langle\Delta\theta(Z)\rangle^t$, respectively. These were converted into reaction times $\langle\tau(Z)\rangle^p$ and $\langle\tau(Z)\rangle^t$ via

$$\langle\tau(Z)\rangle^i = \hbar \cdot \frac{\langle\Delta\theta(Z)\rangle^i}{\langle\dot{\ell}\rangle} \cdot \langle J \rangle$$

with $i=p,t$, $\langle\dot{\ell}\rangle$ representing the mean relative angular momentum during the reaction, and $J=1.3 \cdot J_0$ representing the mean moment of inertia. One can then assign

* now at GSI, Darmstadt

$\langle\tau(Z)\rangle^p,^t$ to the corresponding $K_0^{<, >}(Z)$, and depict K_0 as a function of reaction time (Fig.4). Again, K_0 tends to increase with time. From these results it seems quite unlikely that K_0 reaches an equilibrium value in quasi-fission reactions.

- /1/ B.B.Back et al., Phys.Rev.Lett.46,(1981) 1068
- /2/ M.B.Tsang et al., Phys.Rev.C28,(1983) 747
- /3/ J.Töke et al., Nucl.Phys.A440 (1985) 327
- /4/ K.Lützenkirchen et al., GSI Scientific Report 1984, p.37, and Z.Phys.A320 (1985) 529
- /5/ Th.Døssing and J.Randrup, Phys.Lett.155B (1985) 333
- /6/ K.Lützenkirchen et al., GSI Preprint 85-52 (1985)

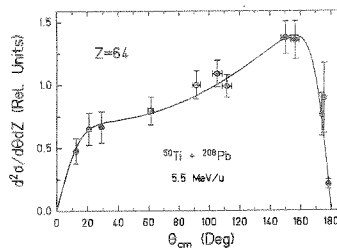


Fig.1: Angular distribution $d^2\sigma/d\theta dZ$ for the target-like quasi-fission fragment $Z=64$.

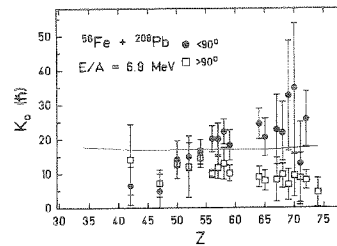


Fig.2: K_0 -values for the forward (\circ) and backward (\square) hemisphere as a function of fragment charge Z.

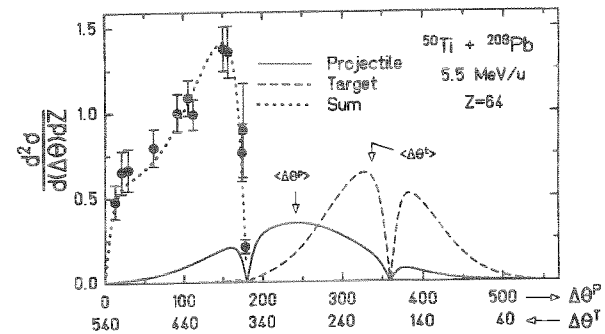


Fig.3: Angular distribution unfolded into a projectile (solid line) and a target (dashed line) contribution depending on the rotation angle $\Delta\theta$. The dotted line results from adding all cross sections in the different $\Delta\theta$ -intervals, and thus corresponds to the measured θ -dependent cross section.

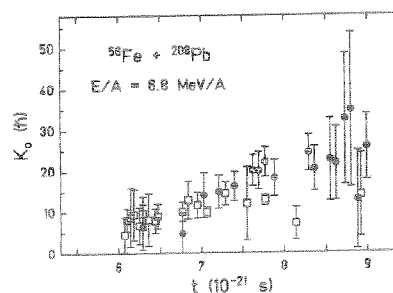


Fig.4: K_0 as a function of time, derived from Fig.2

B
The Tilting Mode in Quasi-Fission Reactions

K. Lützenkirchen* and J.V. Kratz, Institut für Kernchemie der Universität Mainz

G. Wirth, W. Brüche, and K. Sümmerer, GSI Darmstadt

R. Lucas, J. Poitou, and C. Grégoire, DPHN-MF, CEN Saclay

Fission-like reaction products from the interaction of $^{208}_{82}\text{Pb}$ ions with targets of $^{26}_{12}\text{Mg}$ through $^{58}_{26}\text{Fe}$ have previously been studied /1/ with a large position sensitive ring counter. One of the observables was the γ -ray multiplicity, $\langle M_\gamma \rangle$, measured in coincidence with fission-like events. These measurements, however, did not differentiate with respect to the scattering angles.

The mean fragment spin $\langle j \rangle$ was calculated from:

$$\langle j \rangle = 2 \cdot (\langle M_\gamma \rangle - 6) \quad (1)$$

$\langle j \rangle$ is the vector sum of the aligned spin $\langle l_z \rangle$, and the angular momenta corresponding to the six intrinsic rotational modes of a dinucleus. As a working hypothesis the tilting mode, i.e. a common rotation of the fissioning system around the symmetry axis, was considered in /1/ to be the dominant factor. One then obtains:

$$\langle j^2 \rangle \approx \langle l_z^2 \rangle + K_0^2 \quad (2)$$

$\langle l_z \rangle$ can be determined from the mean number of partial waves contributing to the fission cross section /1/. K_0^2 stands for the variance of the angular momenta tied up by the tilting mode. For fissioning compound nuclei K_0^2 is related to the effective moment of inertia at the saddle point via $K_0^2 = T \cdot J_{\text{eff}}$, T being the nuclear temperature. Starting from $\langle M_\gamma \rangle$ one would thus be able to determine nuclear transition-state shapes.

The crucial point, however, is whether it is permissible to interpret $\langle M_\gamma \rangle$ this way (eq.2). If yes there should be a unique connection between the γ -ray multiplicities, $\langle M_\gamma \rangle$, and the angular distributions, $W(\theta)$, and both measurements should lead to the same values of K_0^2 . To test this hypothesis it should be realized that $W(\theta)$ is sensitive to the tilting mode alone, and is not affected by other rotational modes which might possibly be excited, and enter into the $\langle M_\gamma \rangle$ -measurements.

In another contribution to this report /2/ it is described, how K_0 -values near 0° and 180° , $K_0^<$ and $K_0^>$, respectively, can be extracted from skewed angular distributions $d^2\sigma/d\theta dZ$ of the quasi-fission type. Fig.1 depicts K_0 -values as a function of fragment charge Z for the reaction $^{56}\text{Fe} + ^{208}\text{Pb}$ at $E/A = 8.3$ MeV (for details see /3/). In order to allow a comparison of these results with the variances inferred from the angle-integrated $\langle M_\gamma \rangle$, the K_0 -values for $\theta < 90^\circ$ and $\theta > 90^\circ$ had to be formally averaged; this was done with the help of weight factors being related to typical magnitudes of

the cross section near 0° and 180° , respectively. These average values $\langle K_0 \rangle$ are shown as open squares in Fig.2. They all lie clearly below the corresponding variances obtained from $\langle M_\gamma \rangle$ /1/ (dashed line). Thus, eq.2 is incomplete. Other than assumed /1/, all six rotational modes seem to be excited in quasi-fission reactions.

If all six modes contribute equally, then the tilting variance should be of the order of 1/6 of the total one,

$$\sigma_i^2 = 1/6 \cdot \sum_{j=1}^6 \sigma_j^2 \quad (3)$$

with σ_i^2 as the variance of the i -th statistical mode. Using eq.3, revised K_0 -values follow straightforwardly from the $\langle M_\gamma \rangle$ -results (dashed-dotted line in Fig.2). They match the results from $W(\theta)$ almost exactly. The result seems to suggest that, in a quasi-fission reaction, the six modes share the total excitation of intrinsic rotations to roughly equal portions.

- /1/ R. Bock et al., Nucl. Phys. A388 (1982) 334
- /2/ K. Lützenkirchen et al., this report and GSI-Preprint 85-52 (1985)
- /3/ K. Lützenkirchen et al., GSI-Preprint 85-52 and GSI-Report 85-22 (1985)

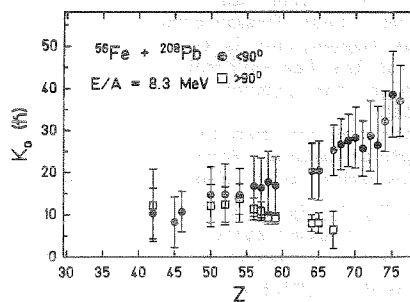


Fig.1: K_0 for the forward (\circ) and backward (\square) hemisphere as a function of fragment charge Z

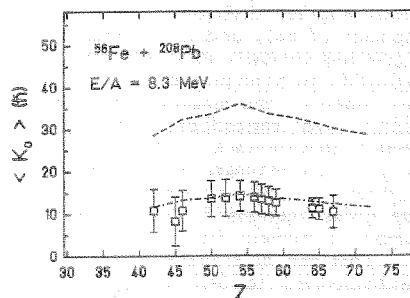


Fig.2: Angle-integrated values $\langle K_0 \rangle$ resulting from $W(\theta)$ (\square). The dashed line is deduced from the sum of the variances of the statistical spins measured via $\langle M_\gamma \rangle$. The dashed-dotted line represents 1/6 of the variances from $\langle M_\gamma \rangle$ (eq.3).

* now at GSI, Darmstadt

Quasi-fission in the $^{40}\text{Ar} + ^{208}\text{Pb}$ reaction near the barrier ^B

H. Keller, K. Lützenkirchen, J.V. Kratz
 Institut für Kernchemie der Universität Mainz
 W. Brüchele, G. Wirth, L. Dörr, E. Jäger
 GSI Darmstadt

Forward-backward asymmetric fission fragment angular distributions in collisions of ^{50}Ti , ^{56}Fe and ^{208}Pb near the barrier have indicated ¹ that only a tiny fraction of these events originate from fission of a completely fused system inside the fission barrier. As predicted by the extra-push model ^{2,3} fusion is replaced in these reactions by a new reaction channel - termed quasi-fission - which approximately equilibrates the mass asymmetry and energy degrees of freedom without ever forming a compound nucleus.

Even for lighter systems such as ^{24}Mg , ^{28}Si and $^{32}\text{S} + ^{208}\text{Pb}$ it was suggested ⁴, based on the observation of unusually large anisotropies, that quasi-fission was contaminating the compound-nucleus fission fragment angular distributions, thus lowering ⁴ the empirical threshold x''_{thr} from about 0.7 ^{5,6} to 0.63. For the intermediate system $^{40}\text{Ar} + ^{208}\text{Pb}$ this new parametrization ⁴ would predict an extra-extra push of the order of 10 MeV, at variance with the results of an analysis ⁵ of evaporation residue cross sections and of the fission excitation function in this reaction, where no evidence for a dynamical hindrance of fusion was found.

We have measured angular distributions of fission-like fragments with specific charges in the $^{40}\text{Ar} + ^{208}\text{Pb}$ reaction at $E_{\text{cm}}=156$ and 172 MeV using catcher foil techniques and K-Xray spectroscopy ⁷. The cross sections $d^2\sigma/dZd\theta$ symmetric around $\theta=90^\circ$ over a wider range of charge numbers as compared to the ^{50}Ti or ^{56}Fe bombardments ⁷, see Fig.1. Nevertheless, with increasing charge asymmetry, left-right asymmetries around $\theta=90^\circ$ become again visible (Fig.1), which prove unequivocally that, even for $^{40}\text{Ar} + ^{208}\text{Pb}$ collisions near the barrier, quasi-fission competes with true compound-nucleus fission. This is corroborated by angular anisotropies for the near-symmetric charge splits that are much larger than predicted by the standard saddle-point model.

Analysis of the angular distributions in the framework of the Randrup-Dössel formalism ⁸ for binary reactions gives values of K_0 depending on the fragment charge (see Fig.2) in a similar way as previously observed for the heavier systems ⁷. Again, for a given value of Z different values of K_0 determined near 0° or 180° , respectively, reflect a different degree of relaxation of the tilting mode for different reaction times.

In order to estimate from the differential angular distributions $d^2\sigma/dZd\theta$ what fraction of the total fission yield is due to compound-nucleus fission we have added to the (skewed) angular distribution of a typical quasi-fission fragment (Z=66), and to its reflection-symmetric image, growing amounts of cross section with an angular distribution as predicted by the standard theory, until the shape of the measured angular distribution near $Z=50$ was reproduced (this approach is similar in spirit to that of Back ⁴). For the $^{50}\text{Ti} + ^{208}\text{Pb}$ reaction this gives an estimate of the order of 10% in reasonable agreement with evidence based on evaporation residue cross sections ². For $^{40}\text{Ar} + ^{208}\text{Pb}$ we estimate a compound nucleus fission contribution of the order of 60%. This can be translated into an extra-extra push (extrapolated to $l=0$) of $E_{\text{xx}}=8\pm 5$ MeV in agreement with Ref.3. The discrepancy with the -0.5 ± 3 MeV figure of Ref.4 might be significant. If so, this would indicate that the assumed equivalence of Coulombic and centrifugal forces, which is used for the extrapolation of the fission data to $l=0$, is at variance with evidence based on evaporation residue cross sec-

tions, where restriction to central collisions is caused by the physical process itself.

- ¹ K. Lützenkirchen et al, Z. Phys. A320, 529 (1985)
- ² W.J. Swiatecki, Physica Scripta 24, T13, (1981)
- ³ S. Bjørnholm, W.J. Swiatecki, Nucl. Phys. A391, 471 (1982)
- ⁴ B. B. Back, Phys. Rev. C31, 2104 (1985)
- ⁵ H. Gäggeler et al., Z. Phys. A316, 291 (1984)
- ⁶ C. C. Sahm et al., Nucl. Phys. A441, 316 (1985)
- ⁷ K. Lützenkirchen et al., Preprint GSI-85-52 (1985)
- ⁸ T. Dössel, J. Randrup, Phys. Lett. 155B, 333 (1985)
- ⁹ F. P. Hessberger et al., Z. Phys. A321, 317 (1985)

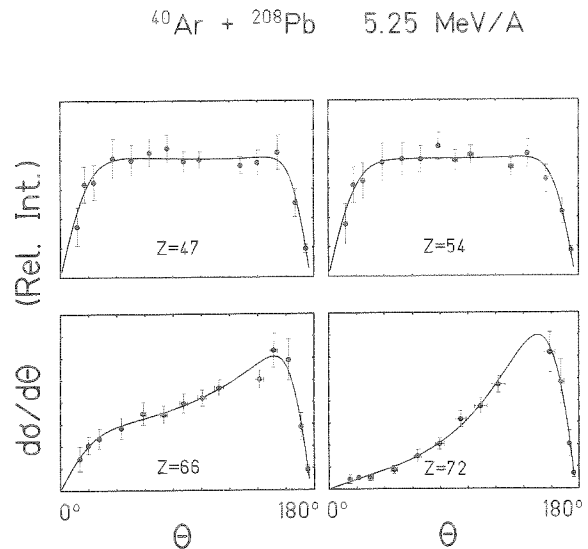


Fig. 1 : Examples for angular distributions $d^2\sigma/dZd\theta$ in quasi-fission reactions of 5.25 MeV/A ^{40}Ar with ^{208}Pb

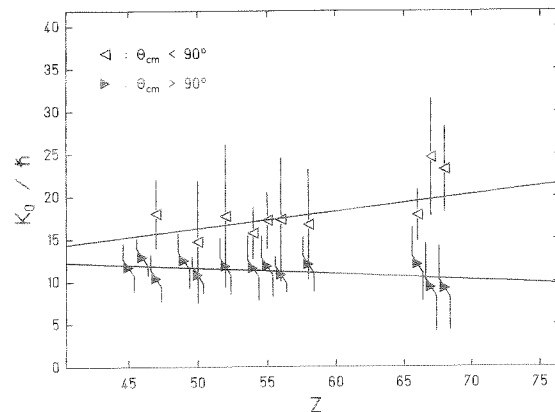


Fig. 2 : Standard deviations K_0 of the distributions of the tilting angular momenta determined from the angular distributions near 0° and 180° as a function of Z.

SEARCH FOR PIONIC FUSION ^B

Th. Blaich, R. Bellwied, J. V. Kratz, S. Zauner
Institut für Kernchemie, Universität Mainz, Germany

W. Brüche, M. Brügger, H. Gäggeler, E. Schimpf
GSI Darmstadt, Germany

S. M. Qaim
Institut für Chemie, KFA Jülich, Germany

Pionic fusion is a very rare exit channel in nuclear reactions in which all the excitation energy is taken away by a pion while the two nuclei fuse in the ground state or a low-lying, particle-bound excited state of the residual nucleus. This process has been observed in reactions between light nuclei, e.g. ${}^3\text{He}({}^3\text{He}, \pi^{-}){}^6\text{Li}$ or ${}^3\text{He}({}^4\text{He}, \pi^{-}){}^7\text{Li}^{12}$, with total reaction cross sections of ≈ 100 nanobarns. With heavier nuclei, the cross sections are expected to be even lower, as the cooperation of all nucleons, required for the transfer of the total excitation energy to a single particle, becomes more and more unlikely. It would, however, be very interesting to find a method sufficiently sensitive to make possible a comparison between the ${}^{207}\text{Pb}({}^4\text{He}, \pi^{-}){}^{211}\text{At}$ - and the ${}^{208}\text{Pb}({}^3\text{He}, \pi^{-}){}^{211}\text{At}$ - cross sections. There exist qualitative estimates based on a microscopic model of pionic fusion³ which predict that the cross section for the pionic fusion of ${}^{207}\text{Pb}$ and ${}^4\text{He}$ should be considerably lower than that for ${}^{208}\text{Pb}$ and ${}^3\text{He}$, due to the similarity between entrance and exit channel in the latter case: both consist of a ${}^{208}\text{Pb}$ -core and three nucleons. Ward et al. investigated the reaction ${}^{208}\text{Pb}({}^3\text{He}, \pi^{-}){}^{211}\text{At}$ and reported cross sections of several nanobarns⁴. We made an attempt to measure the excitation function of the ${}^{207}\text{Pb}({}^4\text{He}, \pi^{-}){}^{211}\text{At}$ - reaction at the isochronous cyclotron JULIC by radiochemical methods. These are best suited for this problem because of their extreme sensitivity.

In preliminary experiments with ${}^{207}\text{Pb}$ (enrichment 92.4%) Astatine was found to be produced below the threshold for pionic fusion, $E = 151$ MeV. It was suspected that this might be due to ${}^{209}\text{Bi}({}^4\text{He}, xn){}^{213-X}\text{At}$ reactions on bismuth impurities on the ppm level. Therefore, excitation functions for these background reactions were measured⁵. Surprisingly, it was found that the isotopic distribution for At produced from ${}^{209}\text{Bi}$ was quite different from that in reactions with ${}^{207}\text{Pb}$ targets, see fig.1. In any case, higher enrichments of ${}^{207}\text{Pb}$ should simultaneously decontaminate from ${}^{209}\text{Bi}$. Therefore the experiments were repeated with a cleaner set of ${}^{207}\text{Pb}$ targets (enrichment 99.81%). Yet, the previous results were reproduced. Since any target contamination must be very long-lived or stable and heavier than lead for the formation of astatine to be possible, one is left with uranium or thorium as further candidates for background reactions. The astatine production cross sections for uranium - measured in the same experiment at 160 MeV - are included in the figure. A contamination of some 10^{16} atoms/cm² of ${}^{235}\text{U}$ could indeed explain our results - if this were not excluded by activation analysis: The targets were irradiated in the Mainz TRIGA-Reactor and searched for ${}^{239}\text{Np}$ and for fission products of ${}^{235}\text{U}$ via γ -ray spectroscopy. We arrive at an upper limit of $2 \cdot 10^{14}$ atoms/cm² for ${}^{235}\text{U}$ which is too low to explain our data. - The significant difference between the isotopic yields of ${}^{207}\text{Pb}$ and ${}^{208}\text{Pb}$ targets also makes an explanation by impurities quite unlikely.

Another possible source of At-isotopes are secondary reactions. The excitation functions for $({}^4\text{He}, xn)$ -reactions range from several millibarns to several hundreds of millibarns, and the $({}^4\text{He}, pxn)$ -cross sections are even larger. As the values are known or can be interpolated with reasonable accuracy, one can collect all possible paths for the production of e.g. ${}^{211}\text{At}$ from ${}^{208}\text{Pb}$ and calculate the secondary yields of At-isotopes. The results are at least an order of magnitude below the measured values. In addition, the isotopic ratios are wrong: As the $({}^4\text{He}, pxn)$ - and $({}^4\text{He}, xn)$ -

cross sections increase with x, secondary reactions favour light isotopes instead of the heavy ones. Reactions of the primary target with a secondary beam, e.g. ${}^6\text{Li}$ produced in $({}^4\text{He}, {}^6\text{Li})$ -reactions, cannot possibly account for the observations either because the $({}^4\text{He}, {}^6\text{Li})$ -reaction by comparison with the $(d, {}^6\text{Li})$ -reaction is estimated to have a cross section of some μbarns .

At present, only a combination of several of the above mentioned effects might serve as an explanation. As the excitation function of ${}^{211}\text{At}$ does not show a significant rise above the threshold for pionic fusion (see fig.2), the upper limit⁶ for the ${}^{207}\text{Pb}({}^4\text{He}, \pi^{-}){}^{211}\text{At}$ - reaction remains at ≤ 30 nanobarns.

References:

1. Le Bornec et al., Phys. Rev. Lett. 47, 1870(1981)
2. Bimbot et al., Phys. Lett. 114B, 311(1982)
3. Huber et al., Nucl. Phys. A396, 191c(1983)
4. Ward et al., Indiana University, Dept. of Chemistry and Cyclotron Facility, Ann. Rep. 1980, p. 63
5. Blaich et al., GSI Scientific Report 1984, GSI 85-1, p. 44

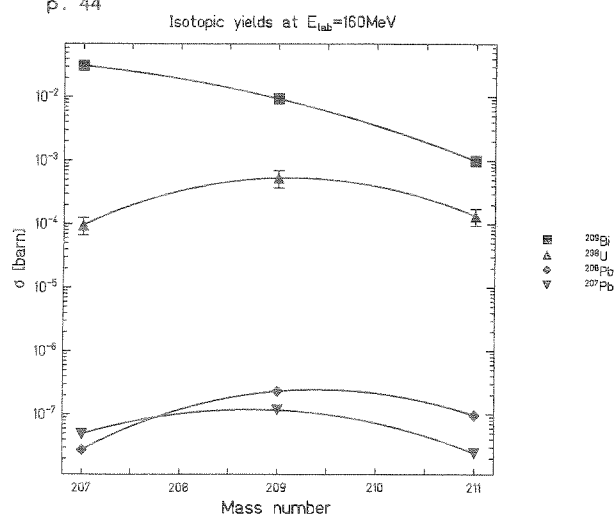


Fig. 1: Isotopic yields of At from different targets at 160 MeV. The lines are drawn to guide the eye.

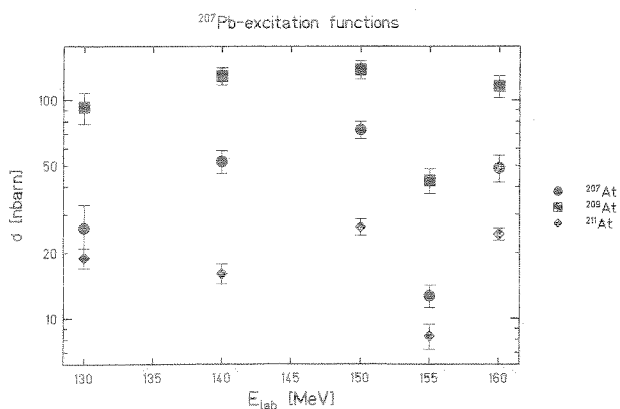


Fig. 2: Excitation functions of At-isotopes from ${}^{207}\text{Pb}$, calculated with the thickness of the lead target.

The irradiation facility at SIS

G. Kraft, B. Fischer, M. Schädel, R. Spohr, H. Stelzer
 GSI Darmstadt
 R. Brandt, Univ. Marburg
 G. Gademann, Univ. Heidelberg

One of the six experimental areas in the 'Target Hall' of the SIS will be dedicated to irradiation experiments of biological, medical and chemical targets as well as for nuclear track experiments. Common to all these experiments is a large area which has to be exposed to a homogeneous flux of ions of up to approx. 10^9 part/sec. In principle, this can be done by two different ways: Active beam scanning by magnetic deflectors and passively, by multiple scattering in foils of heavy elements. The passive scattering has the advantage that a symmetric Gaussian beam distribution is obtained even if the primary beam is fluctuating in intensity over the time. However, to achieve a homogeneous beam spot with less than 10% deviation over an extended area only the inner part of the Gaussian distribution can be used and the outer parts have to be cut off by collimators. Using the passive method, a great amount of nuclear fragments is produced in the scattering foils and of neutrons in the collimators.

A pure beam results only from an active beam scanning using for instance two deflecting magnets perpendicular to the beam axis and to each other. A deflection of ± 0.5 degrees is sufficient to produce the required large beam spot of 20×20 cm² if the wobbler magnets are located more than 12 m upstream. From the accelerator a maximum pulse length of 400 msec with a flat top is proposed. Using a fast power supply with a rise time of 20 msec for the horizontal and a twenty times slower power supply for the vertical deflection one picture will be written within one SIS pulse of 400 msec. In addition to the cleaner beam production, which avoids the nuclear fragmentation, the active beam scanning is able to produce beam sizes of arbitrary shapes and contours.

In order to control the size and homogeneity of the beam spot, position sensitive particle detectors are required. For the low fluxes up to some Mega-Hz low pressure gas filled avalanche counters can be used to measure the position of single particles with a spatial resolution better than 1 mm. For the higher particle fluxes ionisation chambers with different sensitive areas should yield a spatial resolution better than one centimeter.

Another typical problem of the irradiation experiment is a frequent and fast access to the experiment when a set of exposures is done. In order to achieve a quick removal of the activated parts of the beam stop, we want to split the beam catcher into three components: first a block of heavy metal as large as the size of the beam spot and thick enough to stop the primary particles. Secondly, a housing integrated in the rear wall of the shielding material and finally a small neutron catcher located directly behind the experiment.

During the exposure, the metal block surrounded by a neutron catcher will be positioned directly at the experiment. At the end of the exposure only the relatively small metal block has to be transferred to the housing at the rear wall. Using this device, there is no need to transport tons of shielding material after the exposure. In addition, the metal block can be easily changed and used for chemical analysis as proposed by one of us (RB).

The experimental area should have a size of 5×10 m² free for the set-up of different experiments. At least three different exposure apparatuses will be constructed for the experiments, because it is not possible to fulfill the different requirements of biology, chemistry and track research simultaneously. The important beam characteristics summarizes the following list:

- particles: all ions, including the radioaction beam
- intensity: 1 to 1×10^9 part/sec
- energies: 10 MeV/u - 1 GeV/u
- emittance: 5mm x mrad
- time structure: a) slow extraction with a constant intensity over at least 400 msec
 b) fast cut off (≤ 100 µsec)
- collimator: x and y collimators between SIS and the last dipolmagnet
- beam wobbler: two dipol magnets with $\pm 0.5^\circ$ deflection
 12m upstream from the experimental area
 20x20 pixel 400msec per picture
- beam diagnosis: $1-10^9$ particles/sec: low pressure avalanche counters resol. ≤ 1 mm
 10^5-10^9 particles/sec : ionisation chambers with spatial resolution 1-2cm